Shiraz University

Iran Agricultural Research

Journal homepage: https://iar.shirazu.ac.ir/?lang=en

Research Article

Biosynthesis of zinc-based nanoparticles using *Escherichia coli* and *Bacillus subtilis*: Effects on maize (*Zea mays* L.) growth indices and soil microbial activity

Narges Abdar[a], **Mehdi Zarei**[a,c*], **Reza Ghasemi**[a], **Alireza Afsharifar**[b], **Amir Ghaffar Shahriari**[c*]

[a] Department of Soil Science, School of Agriculture, Shiraz University, Shiraz, I. R. Iran
[b] Plant Virology Research Center, School of Agriculture, Shiraz University, Shiraz, I. R. Iran
[c] Department of Agriculture and Natural Resources, Higher Education Center of Eghlid, Eghlid, I. R. Iran

ARTICLE INFO

Keywords:
Biological nanoparticles
Bacillus subtilis
Escherichia coli
Maize
ZnO nanoparticles

Received: 12 February 2026
Revised: 13 May 2026
Accepted: 17 May 2026

ABSTRACT- Biologically synthesized nanoparticles have been considered environmentally friendly agents for improving plant growth in sustainable agriculture. This study aims to evaluate the impacts of biosynthesized zinc oxide nanoparticles (ZnO NPs) on plant growth-promoting rhizobacteria and maize (*Z. mays* L.). ZnO NPs were biosynthesized using *Bacillus subtilis* and *Escherichia coli* with $ZnSO_4$, $Zn(CH_3COO)_2$, and $Zn(NO_3)_2$ as zinc precursors. The morphological properties of the synthesized ZnO NPs were characterized, and their particle sizes ranged from 28 to 600 nm. The results showed that the application of ZnO NPs at 0.1 g L^{-1}, particularly those synthesized using $ZnSO_4$ in the presence of *B. subtilis* and *E. coli*, significantly increased the maize seed germination rate. Basal respiration in the treated soils was also significantly enhanced following the application of 0.5 g L^{-1} $ZnSO_4$ and $Zn(NO_3)_2$ in the presence of *B. subtilis*. Minimum inhibitory concentration (MIC) and minimum bactericidal concentration (MBC) assays showed that ZnO NPs at 0.625 mg mL^{-1} exhibited relatively low bactericidal activity against plant growth-promoting rhizobacteria (PGPR). Chemically synthesized ZnO NPs exhibited the strongest inhibitory activity against PGPR, whereas ZnO NPs that were biosynthesized with *B. subtilis* using $Zn(NO_3)_2$ showed relatively low inhibitory activity at 1.25 mg mL^{-1}. Owing to the greater biocompatibility of biologically synthesized ZnO NPs compared to chemically synthesized ZnO NPs, these materials may serve as promising zinc fertilizers on zinc-deficient soils at relatively low concentrations.

INTRODUCTION

Nanotechnology is an emerging field of science with applications in various areas, including agriculture, pharmaceuticals, wastewater treatment, and soil amendment (Omar et al., 2023). The use of nanomaterials as fertilizers has received considerable attention as a potential approach to promoting sustainable agriculture. Although chemical fertilizers can increase crop productivity, their excessive use can contribute to the soil and water pollution (Spernetto et al., 2020). Therefore, green nanotechnology has emerged as a promising approach for developing environmentally friendly nanofertilizers that can reduce the reliance on conventional chemical fertilizers (Nasrollahzadeh et al., 2019). Nanoparticles (NPs) have also been investigated as potential tools for improving the sustainability of agricultural production (Aslam et al., 2022). Among these, zinc oxide nanoparticles (ZnO NPs) can be synthesized using various biological, chemical, and physical methods (Sabir et al., 2020).

Recently, biological synthesis of NPs has attracted considerable attention because it is a simple, cost-effective, and environmentally friendly approach (Aslam et al., 2022). Bacterial synthesis offers several advantages over other biological methods, including ease of cell manipulation and rapid growth rates (El-Ghwas, 2022; Hamek et al., 2023). Bacteria can synthesize NPs through either extracellular or intracellular mechanisms. The extracellular approach is generally preferred because of its simpler procedure and higher efficiency. Various bacterial species, including *A. hydrophila*, *L. sporogenes*, *P. aeruginosa*, and *B. licheniformis*, have been used for the biosynthesis of ZnO NPs (Ameen et al., 2021; Al-Kordy et al., 2021).

Species of *Bacillus* and *Escherichia coli* have also been widely used for the production of various metabolites and NPs (Sohad et al., 2021; El-Nour et al., 2023). Sohad et al.

*Corresponding Author: Professor, Department of Soil Science, School of Agriculture, Shiraz University, Shiraz, I. R. Iran & Department of Agriculture and Natural Resources, Higher Education Center of Eghlid, Eghlid, I. R. Iran & Associate Professor Department of Agriculture and Natural Resources, Higher Education Center of Eghlid, Eghlid, I. R. Iran
E-mail address: mehdizarei@shirazu.ac.ir & shahriari.ag@eghlid.ac.ir
DOI: 10.22099/iar.2026.55658.1739

(2021) reported that ZnO NPs synthesized by *E. coli* formed white, clustered spherical structures and exhibited an absorption peak at 268 nm. Scanning electron microscopy (SEM) revealed particle sizes ranging from 31.55 to 45.9 nm. El-Nour et al. (2023) used *Bacillus subtilis* ATCC 6633 and $Zn(NO_3)_2$ as the precursor for the biosynthesis of ZnO NPs; transmission electron microscopy revealed spherical particles ranging from 13.5 to 30.4 nm in size. Similarly, Hamek et al. (2023) reported that ZnO NPs biosynthesized by *B. subtilis* ZBP4 using $ZnSO_4$ as the precursor ranged from 22 to 59 nm.

The properties of NPs can vary depending on the bacterial strain used for their synthesis. Furthermore, nanoparticle formation and biosynthesis are strongly influenced by several factors, including pH, reaction time, temperature, and precursor concentration (Fakhari et al., 2019). Of these factors, precursor concentration largely affects nanoparticle biosynthesis (Fakhari et al., 2019).

With the increasing use of ZnO NPs, their residues in the environment are expected to increase continuously (Rizvi and Khan, 2018). Environmental concentrations of ZnO NPs have been reported to range from approximately 100 μg L^{-1} in water to 1 mg kg^{-1} in soil (Garcia-Gomez et al., 2018). Adverse effects on soil microbiota have been observed even at relatively low concentrations (< 1 mg kg^{-1}) (Simonin and Richaume, 2015). Therefore, it is worthwhile to evaluate the effects of ZnO NPs on soil microorganisms.

Most plant growth-promoting rhizobacteria (PGPR) belong to the genera such as *Rhizobium*, *Azotobacter*, *Bradyrhizobium*, *Thiobacillus*, *Bacillus*, *Azospirillum*, *Pseudomonas*, *Burkholderia*, *Arthrobacter*, and *Agrobacterium* (Rizvi and Khan, 2018; Singh et al., 2019; Wilpiszeski et al., 2019). Several studies have investigated the effects of ZnO NPs on beneficial soil microbiota. Ge et al. (2012) reported that ZnO NPs can reduce soil microbial biomass. In addition, soil enzyme activity, an important indicator of the response of plants and microorganisms to environmental stress, can be inhibited by high concentrations of ZnO NPs (Kwak et al., 2017; Garcia-Gomez et al., 2018).

Although most studies have focused on the adverse environmental effects of NPs, fewer have investigated their potential beneficial effects on soil microorganisms. Zinc is an essential element for both soil microorganisms and plants because it is required for the activity of numerous enzymes (Tripathi et al., 2015). Beneficial soil bacteria that promote plant health and increase crop yield may also contribute to the mobilization and availability of micronutrients. In addition to directly affecting plant growth, these bacteria interact with soil and plant microbiomes, which can subsequently influence overall plant health. Therefore, investigating the beneficial interactions between ZnO NPs and soil bacteria is important for understanding their potential applications in sustainable agriculture (Wagner et al., 2016; Duhan et al., 2017).

Maize is the third most important crop worldwide (Ranum et al., 2014). Zinc is an essential micronutrient for maize, and its deficiency can inhibit plant growth and development (Suganya et al., 2020). Seed treatment with zinc is a suitable approach for maize because of its relatively low zinc requirement and the difficulty of applying zinc at the desired concentrations through conventional methods (Umar et al., 2021). Among nanoparticle-based fertilizers, ZnO NPs have been widely investigated; however, their effects on plant growth and yield have been inconsistent (Liu et al., 2015). For example, ZnO NPs concentrations of 400-800 mg kg^{-1} reduced maize yield, whereas a concentration of 500 mg kg^{-1} enhanced soybean growth (Priester et al., 2012; Zhao et al., 2013).

ZnO NPs have also been used as a seed-priming treatment to improve seed germination and alleviate dormancy. They may enhance the growth and productivity of agricultural crops by improving seed growth parameters, increasing vigor indices and growth rates, helping photosynthetic and nitrogen metabolism, and promoting syntheses of carbohydrates and proteins (Ahmadian et al., 2020).

Therefore, this study aimed to (1) synthesize ZnO NPs using *B. subtilis* and *E. coli* with three different zinc salts, i.e., zinc sulfate, zinc acetate, and zinc nitrate, as precursors; and (2) evaluate the effects of the synthesized ZnO NPs on soil respiration and maize growth.

MATERIALS AND METHODS

Plant materials

Maize seeds (*Zea mays* L. cv. SC 704) were obtained from the School of Agriculture, Shiraz University, Shiraz, Iran. The seeds were surface-sterilized with 1% NaOCl and air-dried before cultivation.

Synthesis of ZnO NPs using bacteria

Nutrient broth (NB; Merck, Germany) was inoculated with *Bacillus subtilis* ATCC 6633 (NCBI Taxonomy ID: 703612), provided by the Iranian Research Organization for Science and Technology (IROST), Tehran, Iran, and *Escherichia coli* (NCBI Taxonomy ID: 83333), obtained from the Department of Food Science and Technology, Shiraz University, Shiraz, Iran. The cultures were incubated at 37 °C for 24 h. The cultures were then centrifuged at 10,000 rpm for 10 min to obtain the bacterial supernatants (El-Ghwas, 2022).

ZnO NPs were synthesized using 100 mL of the supernatant from each bacterial culture. The supernatants were mixed separately with 100 mL of 0.5 M zinc salt solutions ($ZnSO_4$, $Zn(NO_3)_2$, and $Zn(CH_3COO)_2$) in 250-mL flasks. The mixtures were heated in a water bath at 80 °C for 10 min, after which 10% KOH was added. The final pH was adjusted to 7.5 using KOH. After removal from the water bath, the formation of a white precipitate indicated the formation of ZnO NPs. The flasks were then incubated on a shaker at 37 °C for 12 h to allow the particles to settle. The ZnO NPs were recovered by centrifugation at 10,000 rpm for 10 min. The precipitates were collected and washed with distilled water, followed by ethanol, to remove residual Zn^{2+} from the particle surfaces. The samples were then dried in an oven at 50 °C for 24 h (Sabir et al., 2020; El-Ghwas, 2022; Hamek et al., 2023; El-Nour et al., 2023).

Characterization of ZnO NPs

The synthesized ZnO NPs were characterized using UV–Visible spectroscopy, transmission electron microscopy,

Fourier-transform infrared spectroscopy, and dynamic light scattering, following methods by Sabir et al. (2020).

UV–Visible spectroscopy

ZnO NPs were suspended in sterile distilled water at a concentration of 5 mg per 20 mL. The maximum absorbance was recorded over the wavelength range of 300–700 nm using a Lambda 365 spectrophotometer (PerkinElmer, USA).

Transmission electron microscopy (TEM) analysis

ZnO NP suspensions (100 mg mL^{-1}) were prepared at the Plant Virology Research Center, School of Agriculture, Shiraz University, Shiraz, Iran. A 10-µL aliquot of each suspension was dropped onto a copper grid and air-dried. TEM images were obtained using a CM-10 transmission electron microscope (Philips, Netherlands).

Fourier-transform infrared spectroscopy (FTIR) analysis

KBr powder and ZnO NPs were mixed at a ratio of 100:1 (KBr:ZnO NPs) and pressed into a 2-mm semi-transparent disk. The samples were analyzed using a Tensor II FTIR spectrophotometer (Bruker, Germany) over the range of 4000–400 cm^{-1}.

dynamic light scattering (DLS) analysis

The particle-size distribution of the ZnO NPs was determined using an SZ-100 DLS instrument (HORIBA, Japan) at a scattering angle of 90° and room temperature. Approximately 2 mg of each NP sample was suspended in 6 mL of DSW before analysis.

Germination and growth of maize

Ten maize seeds from each treatment were placed in 9-cm Petri dishes containing Whatman No. 42 cellulose filter paper. The treatments consisted of a control (C0), in which seeds were treated with DSW, and three ZnO NP concentrations: 0.1 (C1), 0.5 (C2), and 1.0 (C3) g L^{-1}. Each treatment was replicated three times. Ten mL of each ZnO NP suspension was applied to the seeds using a sterile syringe. The Petri dishes were incubated in a growth chamber at 20 ± 1 °C for one week.

Soil basal respiration

A factorial experiment with three replicates was conducted using a completely randomized design (CRD). ZnO NPs were applied to the soil at concentrations of 0, 0.1, 0.5, and 1.0 g kg^{-1} soil. Six types of biologically synthesized ZnO NPs were evaluated: $ZnSO_4$-*B. subtilis* (ZSB), $Zn(NO_3)_2$-*B. subtilis* (ZNB), $Zn(CH_3COO)_2$-*B. subtilis* (ZAB), $ZnSO_4$-*E. coli* (ZSE), $Zn(NO_3)_2$-*E. coli* (ZNE), and $Zn(CH_3COO)_2$-*E. coli* (ZAE). A chemically synthesized ZnO NPs formulation (20–30 nm) was also included. Soil samples were collected from a depth of 0–30 cm. The ZnO NPs were dispersed in sterile distilled water and thoroughly mixed with the soil. Fifty grams of moist soil, adjusted to 100% field capacity, was placed in a glass container and incubated at 25 °C. A total of 84 samples were prepared and incubated for seven days. Soil basal respiration was determined according to Huang et al. (2021). Carbon dioxide (CO_2) released from the soil was absorbed in 0.05 M sodium hydroxide (NaOH) solution and subsequently precipitated as barium carbonate ($BaCO_3$) by adding 0.5 M barium chloride ($BaCl_2$). The remaining NaOH was titrated with 0.1 M hydrochloric acid (HCl) using phenolphthalein as an indicator, and the amount of CO_2 released was calculated.

Minimum inhibitory concentration (MIC) and minimum bactericidal concentration (MBC) assays

The bacterial species *Bacillus subtilis*, *Azospirillum* sp., *Pseudomonas fluorescens*, and *Micrococcus yunnanensis* were obtained from the Department of Soil Science, Shiraz University, Shiraz, Iran. ZnO NPs were dispersed in nutrient broth at concentrations of 10, 5, 2.5, 1.25, and 0.625 mg mL^{-1}. One milliliter of each bacterial suspension, adjusted to approximately 10^8 CFU mL^{-1}, was added to the respective ZnO NP treatments. The cultures were incubated at 37 °C for 24 h. Bacterial growth was evaluated visually by observing turbidity and by measuring optical density at 600 nm (OD_{600}). To determine the MIC, the lowest ZnO NP concentration that prevented visible bacterial growth was recorded as the MIC. To determine the MBC, samples from tubes showing no visible growth were streaked onto nutrient agar plates and incubated at 37 °C for 24 h. The MBC was defined as the lowest ZnO NPs concentration at which no bacterial colonies developed on the agar plates (Chikezie et al., 2017).

Statistical analysis

Statistical analyses were performed using SAS version 9.2 and GraphPad Prism version 9.5. Two-way general linear models (GLM) were used for evaluating the effects of the experimental factors and their interactions. Multiple comparisons were performed using Duncan's multiple range test ($P < 0.05$).

RESULTS AND DISCUSSION

Properties of ZnO NPs

Since the biological synthesis of NPs is more environmentally friendly than conventional chemical synthesis (Sabir et al., 2020), ZnO NPs were synthesized using *B. subtilis* and *E. coli*. The formation of a white pellet indicated that both bacterial strains were able to synthesize ZnO NPs using zinc sulfate, zinc nitrate, and zinc acetate as precursors. The UV–Vis absorption spectra of the synthesized ZnO NPs are presented in Fig. 1. The absorption maxima were observed at 347, 276, 362, 347, 398, and 385 nm for ZNE, ZSE, ZAE, ZNB, ZSB, and ZAB NPs, respectively. Overall, the UV–Vis spectra showed absorption in the range of approximately 350–400 nm, which is consistent with the characteristic absorption range reported for ZnO NPs. Previous studies have reported absorption peaks at 380 nm (Khana et al., 2019; Mohd Yusof et al., 2019), 340–385 nm (Hudlikar et al., 2012), and 368 nm (Singh et al., 2019). Almoneef

et al. (2024) also reported an absorption peak at 283 nm for ZnO NPs. According to Singh et al. (2012), changes in nanoparticle size can cause shifts in the absorption peak toward either shorter or longer wavelengths. Also, a decrease in the intensity of the absorption band may indicate limited aggregation of the NPs (Sánchez-Pérez et al., 2023). Singh et al. (2012) reported an absorption peak at 361 nm for ZnO NPs with a particle size of approximately 40 nm. Therefore, variations in particle size may account for the differences observed in the absorption maxima among the synthesized ZnO NPs.

The findings indicated that the intensity of the SPR peak varied depending on the type of Zn salt and bacteria used for NP synthesis. The DLS results showed that the size ranges of ZNE, ZSE, ZAE, ZNB, ZSB, and ZAB were 27.9–33, 588–677, 94.4–110.1, 99.6–117, 51.3–60.8, and 173.4–191.7 nm, respectively (Fig. 2). In most studies, the size of ZnO NPs ranges from 40 to 75 nm; however, the results of our research showed that the size of ZnO NPs ranged from 28 to 200 nm. Khajeh and Golzari (2014) also synthesized ZnO NPs with sizes ranging from 11 to 25 nm. Previous studies have reported biologically synthesized ZnO NPs using *P. aeruginosa* (35–80 nm, globular), *Lactobacillus* spp. (30–38 nm), and *B. subtilis* (16–20 nm, spherical and non-aggregated), which are consistent with our findings (Salman et al., 2018; Singh et al., 2019). Moreover, TEM results showed that the particles were mainly spherical and dispersed, with sizes ranging from 20 to 80 nm (Fig. 3).

DLS is one of the most common techniques used to determine the distribution of particle sizes in a colloidal solution based on intensity. Mohmed et al. (2019) reported that the particle sizes obtained by DLS were larger than those measured using TEM because the size obtained by DLS is not only related to the metallic core of the particles but is also influenced by the capping proteins and enzymes surrounding the particles (Mohmed et al., 2019).

On the other hand, selecting a Zn salt precursor has a substantial impact on the reaction outcomes, provided that the precipitation conditions remain unchanged. A considerable degree of agglomeration was observed in all NPs, suggesting that the salt precursor was ineffective in maintaining the separation of individual grains. Various zinc metal salts, including $Zn(CH_3COO)_2{\cdot}2H_2O$, $Zn(NO_3)_2{\cdot}6H_2O$, $ZnCl_2$, and $ZnSO_4{\cdot}H_2O$, contain distinct counter anions, such as NO_3^-, CH_3COO^-, Cl^-, and SO_4^{2-}. These anions are important because their electrostatic stabilization abilities vary among salts; therefore, this difference is expected to affect the size and morphology of NPs (Pourrahimi et al., 2014). Anions with strong stabilizing properties, such as CH_3COO^-, can attach to expanding crystal surfaces during a reaction, thereby hindering crystal growth and leading to the formation of smaller NPs. In contrast, anions such as SO_4^{2-}, which have no stabilizing properties, lead to the formation of larger NPs (Pourrahimi et al., 2014).

In addition to the stabilizing properties of the anions, it has been observed that morphology and growth rate are also affected by the interaction between the K^+ cation from KOH (the precipitating agent used during biosynthesis) and the various counter anions (Nkabinde et al., 2018). Notably, researchers have utilized the limited capacity of NO_3-based precursors to inhibit the movement and aggregation of smaller particles in various scientific investigations focused on developing specific directional morphologies in hydroxide solutions. The kinetics of growth and variation in particle size have previously been associated with the "virtual" capping shells formed by cations from alkaline sources such as KOH (Singh et al., 2023).

On the other hand, FTIR was used to identify ZnO NPs synthesized using *B. subtilis* and *E. coli*. Similar bands were observed in the FTIR spectra of ZNE and ZSE, positioned at 3300–3307, 1639–1640, 1119, 1046, 960–961, and 599 cm^{-1} (Fig. 4b). The bands observed at 3307, 1640, 1119, 1046, and 961 cm^{-1} resulted from the presence of O–H groups, C=O stretching in proteins, C–O stretching groups in ethers, C–O–C bending vibrations, and N–O amine oxide, respectively. The vibrational frequencies at 599 and 542 cm^{-1} in this region were attributed to the ZnO (Fig. 4b).

The FTIR spectra of ZAE, ZAB, and ZNB also showed similar bands positioned at 3368–3386, 1554, 1392–1394, 1334–1335, 1019–1020, 828–829, 672, and 542 cm^{-1} (Fig. 4a and Fig. 4b). Therefore, it is likely that ZnO NPs produced through biosynthesis contain an organic group similar to a protein, which functions to form a corona and maintain the stability of the NPs. The FTIR results confirmed the presence of C=O groups from acid amino residues, which may arise from metal NPs in proteins, indicating a strong ability of proteins to bind metals specifically. The dual function of metal NPs is involved in their formation and removal (Salman et al., 2018).

The wavelength of ZnO NPs was 519 cm^{-1} (Raj and Lawerence, 2018). As a result, a white precipitate of ZnO NPs was obtained from a new bacterial strain of *B. subtilis* and *E. coli*. FTIR studies indicate that the presence of various bioactive functional groups in bacteria facilitates the formation and stabilization of NPs (Singh et al., 2023). The anticipated process of NPs biosynthesis by microorganisms is based on enzymatic activity. As a result, enzymes, glycosides, saponins, and various other biomolecules may contribute to the stabilization of NPs (Solís-Sandí et al., 2023).

Research findings suggest that the addition of metal salts to the bacterial supernatant results in Zn ions interacting with proteins and water-soluble substances through –OH and –COOH groups, causing structural alterations in the protein molecules. These changes facilitate the conversion of the bound metal ion into ZnO NPs (Yadav et al., 2023).

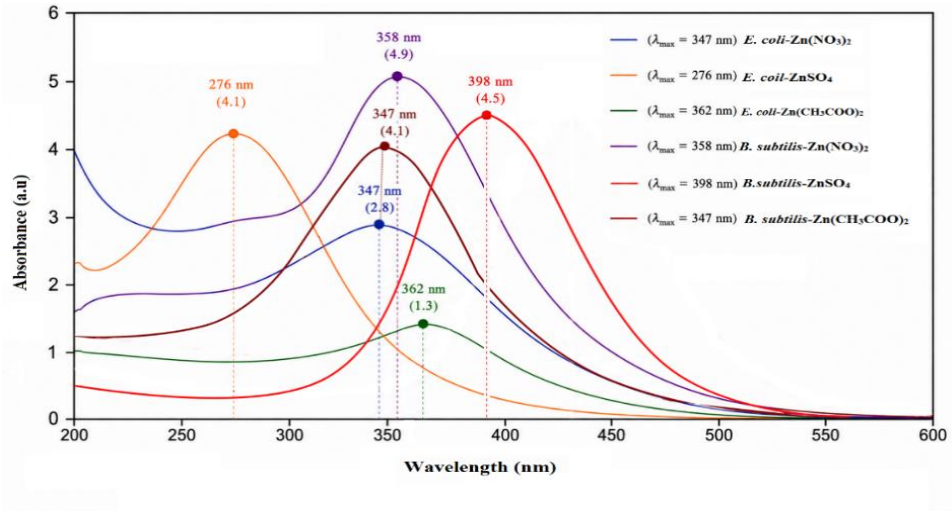

Fig. 1. UV-Visible spectrum of biologically synthesized ZnO NPs using *Bacillus subtilis* and *Escherichia coli* with three Zn salts ($ZnSO_4$, $Zn(NO_3)_2$, and $Zn(CH_3COO)_2$).

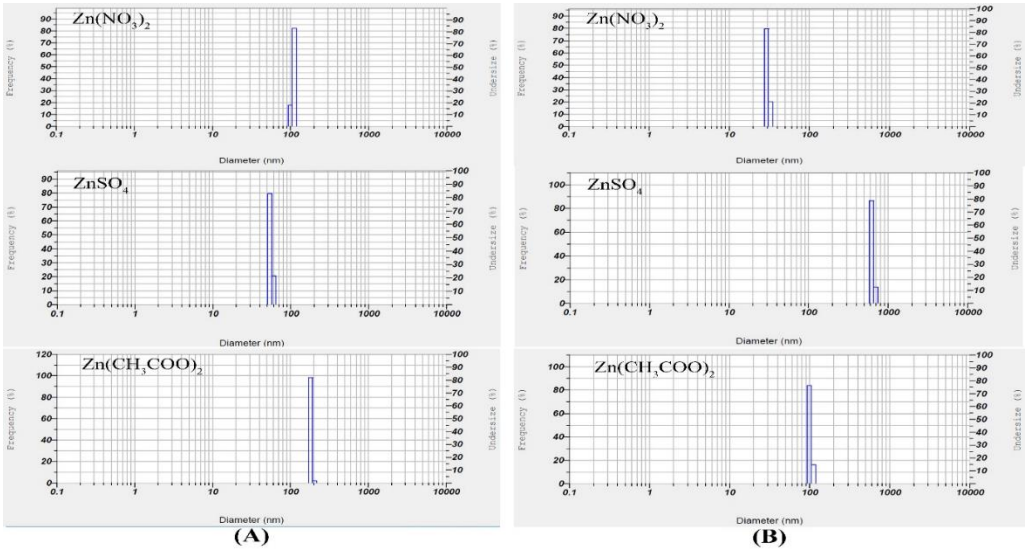

Fig. 2. Dynamic light scattering of ZnO NPs biologically synthesized by (a) *Bacillus subtilis* and (b) *Escherichia coli*.

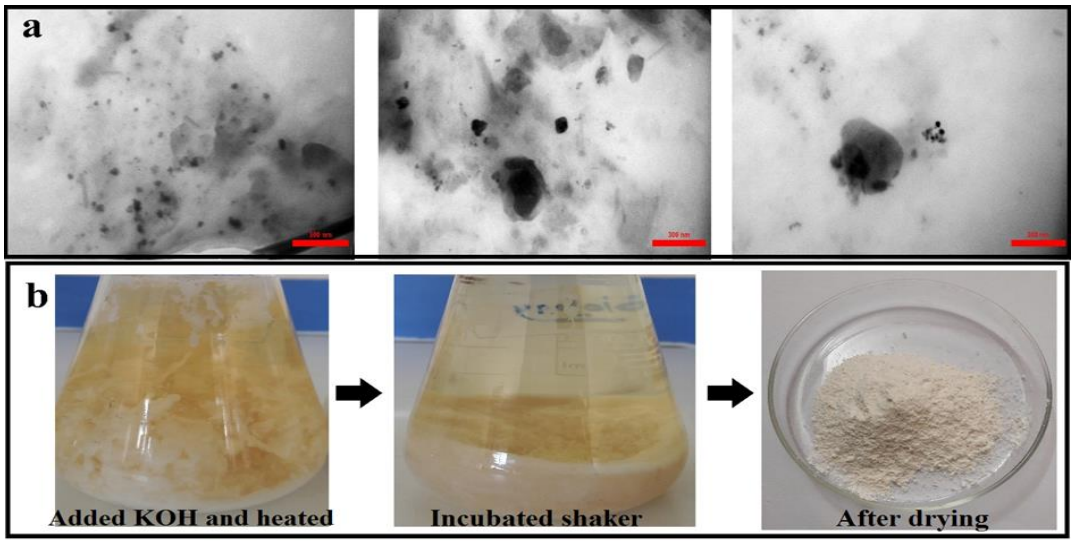

Fig. 3. (a) Transmission electron microscopy of ZnO NPs biologically synthesized by *Escherichia coli* including $Zn(NO_3)_2$-*E. coli* (left), $ZnSO_4$-*E. coli* (middle), and $Zn(CH_3COO)_2$-*E. coli* (right). (b) The experimental process of ZnO NPs synthesis including the heat and KOH addition to bacterial and Zn salt suspension (left), precipitation of ZnO NPs using incubation shaker (middle), and oven-dried pellet containing the ZnO NPs (right).

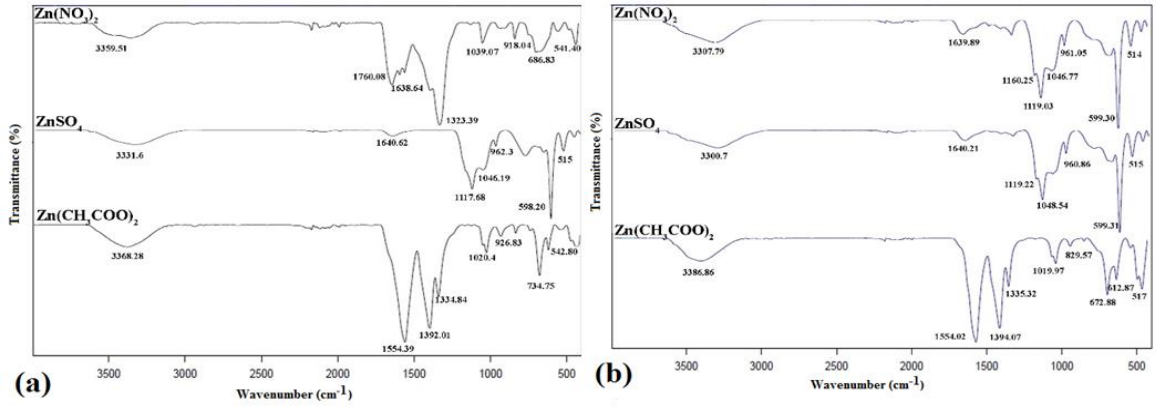

Fig. 4. Fourier-transform infrared spectroscopy of ZnO NPs biologically synthesized using (a) *Bacillus subtilis* and (b) *Escherichia coli.*

Effect of ZnO NPs on maize seed

According to the statistical analysis, the effects of ZnO NPs type, concentration level, and the ZnO NPs × concentration level interaction on the germination speed index (GSI), seedling dry weight (SDW), and root dry weight (RDW) examined in this study were significant at the 1% probability level ($P < 0.01$) (Table 1). The results showed that increasing concentrations of ZAB and ZAE were significantly associated with a decrease in GSI. Moreover, treatment with ZSE and ZSB at 0.1 g L^{-1} significantly increased GSI by 14.88% and 15.15%, respectively, whereas treatment with ZSB at 0.5 g L^{-1} significantly decreased GSI by 31.3% compared to the control (Fig. 5a and Fig. 6). The highest increase in GSI was observed when ZSB and ZSE were applied at a concentration of 0.1 g L^{-1}, with values of 8.25 and 9, respectively (Fig. 5a and Fig. 6).

Application of ZnO NPs synthesized by *B. subtilis* and *E. coli* significantly increased maize SDW regardless of the Zn sources (Fig. 5b). At a concentration of 1 g L^{-1}, ZAE, ZAB, ZSB, and ZSE significantly decreased RDW by 58.58%, 29.75%, 57.96%, and 49.52%, respectively (Fig. 5c and Fig. 6). Treatment with ZAE at 0.1 and 0.5 g L^{-1} significantly increased RDW compared to the control by 19.89% and 18.94%, respectively (Fig. 5c and Fig. 6). Treatment with ZNE and ZNB at different concentrations did not show any significant differences in GSI or RDW compared to the control (Fig. 5a, Fig. 5c, and Fig. 6).

The highest increases in SDW and RDW were observed in treatments with ZAE at 0.1 g L^{-1} (35.21% and 19.89%, respectively), compared to the control, whereas the lowest SDW and RDW values were found at all concentrations of chemically synthesized ZnO NPs. The values of SDW and RDW obtained with chemically synthesized ZnO NPs were significantly lower than those obtained with biologically synthesized ZnO NPs (Fig. 5b, Fig. 5c, and Fig. 6).

This study was conducted to evaluate the effects of ZnO NPs type and concentration on plant growth. The findings of this study indicated that a concentration of 0.1 g L^{-1} ZnO NPs is optimal for enhancing the root and shoot lengths of maize seedlings. In contrast, higher concentrations resulted in a reduction in these parameters. Esper Neto et al. (2020) reported that the application of ZnO NPs suspensions at doses of 70–100 mg L^{-1} for maize seed priming resulted in a remarkable enhancement of germination rate, vigor, root length, and the overall production of fresh and dry biomass (Esper Neto et al., 2020). Srivastav et al. (2019) reported a similar result. Nevertheless, an increased concentration of ZnO NPs, specifically 200 mg L^{-1}, led to a reduction in root and shoot lengths (Fakhri et al., 2019). Consequently, increasing the Zn concentration was favorable for plants and contributed to the improved growth. Toxicity was observed at elevated ZnO NPs concentrations (150–200 mg L^{-1}), which might be attributed to the disruption of zinc homeostasis and indirect effects on the uptake of other elements, as well as interactions among these elements (Fakhri et al., 2019). The addition of ZnO NPs to maize seeds led to a significant increase in various growth parameters. SDW and RDW increased in plants treated with ZAE at a dose of 0.1 g L^{-1} by 35.21% and 19.89%, respectively, compared to the control.

According to Munir et al. (2021), seed priming with ZnO NPs resulted in a higher Zn concentration in the roots and shoots compared to the control. Singh et al. (2023) compared chemically synthesized ZnO NPs (48 nm) with biologically synthesized ZnO NPs (35 nm) and found that higher growth rates, in terms of shoot and root length, were obtained through the biological synthesis of ZnO NPs, which was attributed to the smaller diameter of the NPs. Similarly, our results showed that the use of bacteria in ZnO NPs biosynthesis resulted in improved growth parameters compared to the chemically synthesized ZnO NPs.

Sanchez-Perez et al. (2023) reported that ZnO NPs produced through biosynthesis enhanced the germination rate, whereas chemically synthesized NPs reduced seed germination at high doses. Biological ZnO NPs are more efficient in producing bioactive compounds and stimulating enzymes due to their superior biocompatibility (Sánchez-Pérez et al., 2023). These NPs demonstrated greater efficacy in stimulating plant defense mechanisms and enhancing the levels of bioactive compounds and enzymatic activity, even at lower doses, compared to the chemically synthesized NPs (Sánchez-Pérez et al., 2023).

Based on the results, ZnO NPs biologically synthesized using different Zn sources can be applied as a seed-priming agent, leading to the improved germination rates and enhanced seedling growth. Therefore, ZnO NPs can serve as a fertilizer for maize growth at low doses. A separate study demonstrated that ZnO NPs enhance phytohormones, including indole-3-acetic acid in roots, as well as grain germination, vigor index, photosynthetic activity, N metabolism, and the synthesis of carbohydrates and proteins (Sarkhosh et al., 2022). Zn typically serves as a catalytic

metal for enzymes and is also involved in the synthesis of tryptophan and auxins (Almoneef et al., 2024).

Effects of ZnO NPs on soil biological activity

In addition to their considerable effects on plant life, ZnO NPs have also been documented to influence bacterial growth. The cytotoxicity of NPs toward beneficial soil bacterial strains depends on a series of factors, including the morphology, dimensions, chemical composition, and concentration of the NPs, as well as the duration of exposure (Ameen et al., 2021). Our results showed that the MIC and MBC of ZnO NPs for PGPR were effective at dilutions higher than 0.625 mg mL^{-1}. On the other hand, ZnO NPs showed lower antimicrobial activity against *M. yunnanensis* and *B. subtilis* (with ZnO NP biosynthesis by *E. coli*). chemically synthesized ZnO NPs had the greatest ability to inhibit PGPR growth (Table 2 and Fig. 7).

According to a study conducted by Munir et al. (2018), four PGPR species, including *B. thuringiensis*, *P. mosselii*, *A. chroococcum*, and *S. meliloti*, were sensitive to less than 1500 µg mL^{-1} of ZnO NPs. ZnO NPs toxicity is probably a function of (1) cessation of bacterial cellular respiration and (2) oxidative damage and cell lysis (Ahmad et al., 2020). Moreover, by damaging cells and reducing cell viability, NPs also impede the synthesis of certain bioactive molecules that are essential for plant growth and soil fertility. For example, different doses of ZnO NPs decreased IAA production in three PGPR strains, and at a dose of 1000 µg mL^{-1}, the substance was completely eliminated. The observed decrease in IAA synthesis could be linked to slow bacterial growth and the physiological alterations induced by NP stress. The antimicrobial action of oxide NPs is likely attributed to the release of Zn^{2+} and the generation of reactive oxygen species (ROS), which ultimately leads to the cellular membrane damage (Zhang et al., 2018).

Differences were observed among samples treated with different ZnO NPs types in the MIC and MBC assays (Table 2; Fig. 7 and Fig. 8), using *M. yunnanensis*, *P. fluorescens*, *Azospirillum*, and *B. subtilis*. Following a 24 h aerobic incubation period at 37 °C, turbidity was observed in all test tubes containing 0.625 mg mL^{-1} of ZnO NPs, indicating bacterial growth. No turbidity was observed at doses of 1.25, 2.5, 5, and 10 mg mL^{-1} (Table 2; Fig. 7 and Fig. 8). After culturing on nutrient agar (NA) plates and incubating at 37 °C for 24 h, no *Azospirillum* growth was observed at 10 mg mL^{-1} of ZNE, ZAE, ZNB, and ZAB (Fig. 7, Fig. 8A(b), and Fig. 8C(b)). The MBC test at various concentrations showed that *B. subtilis* exhibited significant growth inhibition when exposed to 1.25 mg mL^{-1} of ZNE, 5 mg mL^{-1} of ZAE and ZNB, and 10 mg mL^{-1} of ZSE, ZAB, and chemically synthesized ZnO NPs (Table 2). The 0.625 mg mL^{-1} dose of ZnO NPs showed relatively low bactericidal activity against PGPR (Table 2). The antibacterial effects of the different ZnO NPs types on PGPR were ranked as follows: chemically synthesized ZnO NPs > ZSE > ZSB > ZNE > ZAE > ZAB > ZNB.

The results showed that chemically synthesized ZnO NPs had the highest ability to inhibit PGPR growth (Fig. 7D). Thus, ZnO NPs showed greater antimicrobial activity against *M. yunnanensis* and *B. subtilis* (Table 2). The effectiveness of ZnO NPs against PGPR at concentrations greater than 0.625 mg mL^{-1} was confirmed by both the MIC and MBC results (Table 2). The antimicrobial effect depends on the type of NPs and the microorganism. Research has shown that the MICs of ZnO NPs biosynthesized by *B. haynesii* and *Acinetobacter schindleri* SIZ7 against *E. coli* were 8 and 0.1 mg mL^{-1}, respectively, while those against *S. aureus* were 4 and 0.2 mg mL^{-1}, respectively (Siddhardha et al., 2016; Thakur et al., 2021).

The antibacterial activity of ZnO NPs at different doses was assessed against Gram-negative bacteria, such as *Azospirillum* and *P. fluorescens*, as well as Gram-positive bacteria, such as *M. yunnanensis* and *B. subtilis* (Fig. 7). The MIC of ZnO NPs was 2.5 and 5 mg mL^{-1} against *B. subtilis* for ZnO NPs biosynthesized using *B. subtilis*, 5 mg mL^{-1} against *Azospirillum*, and 1.25 and 2.5 mg mL^{-1} against *P. fluorescens*. The growth ability of *M. yunnanensis* exposed to different concentrations of ZnO NPs was greater than that of the other bacteria. Hamke et al. (2023) reported that the inhibition zone measured for Gram-negative bacteria was greater than that for Gram-positive bacteria because the cell wall of Gram-positive bacteria has a thicker peptidoglycan layer than that of Gram-negative bacteria (Rehman et al., 2019).

ZnO NPs injure cell membranes and enter cells, where they generate ROS and destroy cellular contents (Ali et al., 2018). This was consistent with the results obtained in our study. Thus, in the present study, to determine the potential harmful effects of ZnO NPs, the sensitivity of some beneficial soil bacterial species to the synthesized NPs was investigated using MIC and MBC tests. However, MIC and MBC values obtained in NB medium may not be directly extrapolated to the natural soil systems. In soils, the presence of clay and organic matter can further adsorb NPs or increase their heterogeneous aggregation, which generally reduces their mobility and toxicity compared to the liquid culture conditions. Therefore, although our MIC/MBC results provide a useful basis in a simplified system, they should be interpreted with caution when predicting the environmental behavior or ecological risks of nano-ZnO NPs in complex matrices such as soil. Therefore, the effect of ZnO NPs on soil basal respiration was also investigated.

Table 1. The variance analysis of different parameters in this study

Source	df	Mean of squares							
		SDW		RDW		GSI		SBR	
ZnO NPs	6	0.0039**	$P = 0.01$	0.012**	< 0.001	9.69**	< 0.001	165.88**	< 0.001
Concentrations	3	0.0022**	< 0.001	0.012**	< 0.001	9.7**	< 0.001	151.77**	< 0.001
ZnO NPs × Concentrations	18	0.0006**	< 0.001	0.002**	< 0.001	1.97**	< 0.001	66.36**	< 0.001
Error	56	0.00013		0.0004		0.26		3.89	
CV	-	10.77		16.28		7.78		14.07	

* Probability level at 1%, ** probability level of 5%, df: degrees of freedom, ns: no significant, ZnO NPs: zinc oxide nanoparticles, CV: coefficient of variance, SDW, seedling dry weight, RDW: root dry weight, GSI: germination speed index and SBR: soil basal respiration.

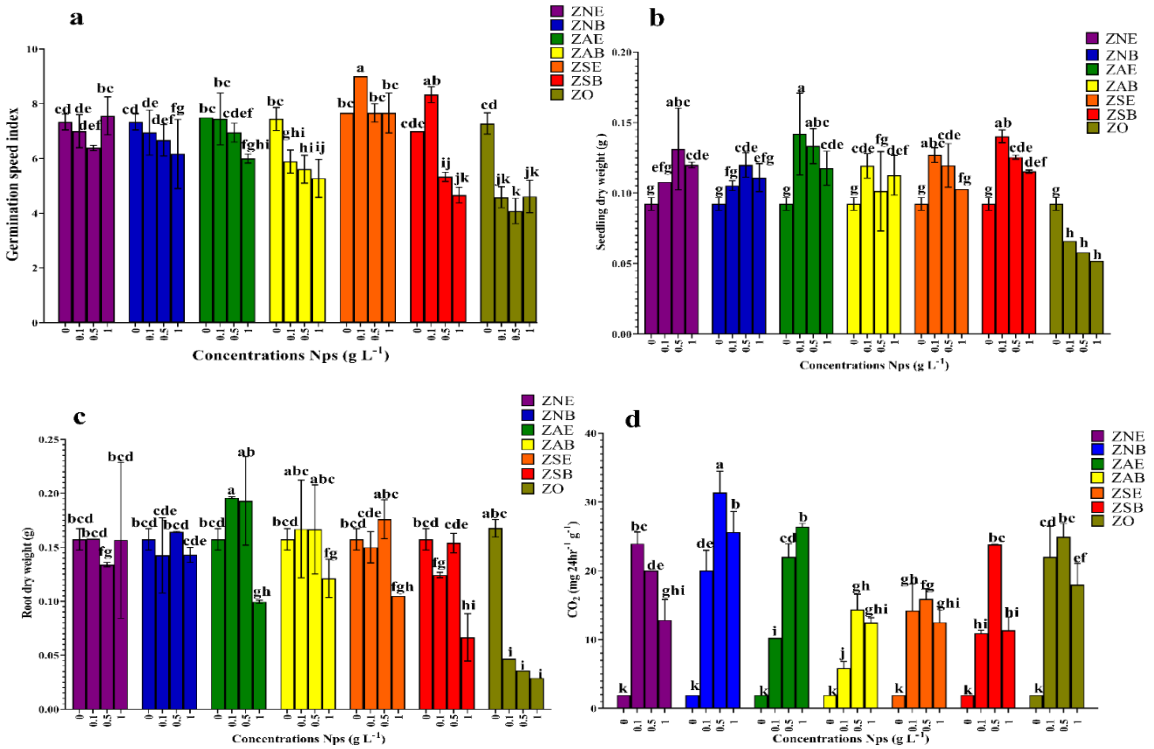

Fig. 5. (a) Germination speed, (b) seedling weight (g), (c) root weight (g), and (d) soil basal respiration (mg CO_2 24 h^{-1} g^{-1}) under various levels of ZnO NPs. ZNE: Zn $(NO_3)_2$-*Escherichia coli*, ZNB: Zn$(NO_3)_2$-*Bacillus subtilis*, ZAE: Zn$(CH_3COO)_2$-*Escherichia coli*, ZAB: Zn $(CH_3COO)_2$-*Bacillus subtilis*, ZSE: $ZnSO_4$-*Escherichia coli*, ZSB: $ZnSO_4$-*Bacillus subtilis*, ZO: chemically synthesized ZnO NPs.

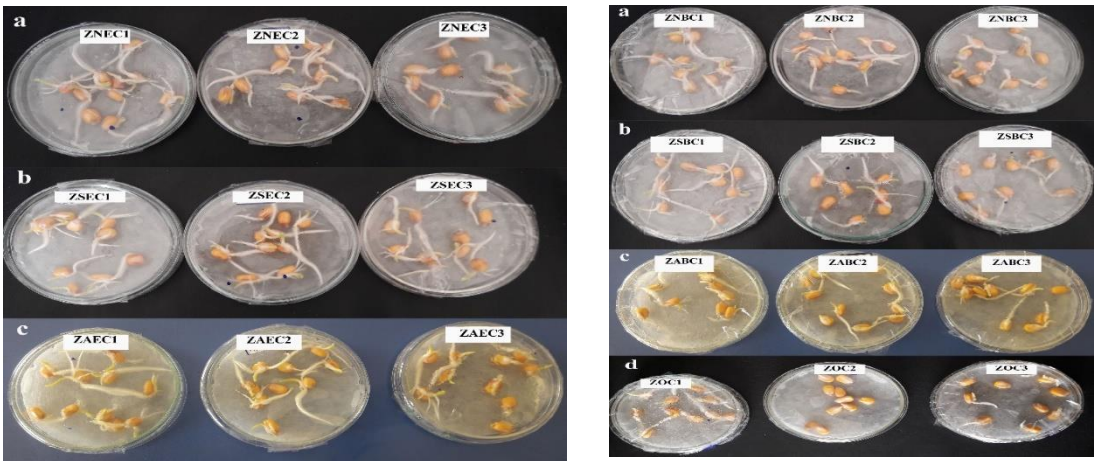

Fig. 6. The photographs illustrate how the different concentrations of ZnO NPs (C_1: 0.1 g L^{-1}, C_2: 0.5 g L^{-1}, and C_3: 1 g L^{-1}) affect maize seed germination when treated with the following nanoparticle types: (a) ZNE (*Escherichia coli*–Zn$(NO_3)_2$), (b) ZSE (*Escherichia coli*–$ZnSO_4$), (c) ZAE (*Escherichia coli*–Zn$(CH_3COO)_2$), (d) ZNB (*Bacillus subtilis*–Zn$(NO_3)_2$), (e) ZSB (*Bacillus subtilis*–$ZnSO_4$), (f) ZAB (*Bacillus subtilis*–Zn$(CH_3COO)_2$), and (g) ZO (chemically synthesized ZnO).

Variance analysis showed that the effects of ZnO NPs type, concentration level, and the ZnO NPs × concentration level interaction on soil basal respiration (SBR) examined in the study were significant ($P < 0.01$) (Table 1). SBR increased remarkably in all treatments compared to the control (Fig. 5d). The other treatments had lower respiration rates than the 0.5 g L^{-1} ZNB treatment (Fig. 5d). Peak values for CO_2 emission rates were reached at 0.5 g L^{-1} ZNB, ZSB, and ZAB (31.39, 23.82, and 14.36 mg 24 h^{-1} g^{-1}, respectively). These values then declined at a concentration of 1 g L^{-1} for ZNB, ZSB, and ZAB by 18.28%, 52.35%, and 13.23%, respectively (Fig. 5d). Treatment with 0.1 g L^{-1} ZNE stimulated SBR (23.46 mg 24 h^{-1} g^{-1}), and SBR was significantly higher compared to the other ZnO NPs. However, the addition of 0.5 and 1 g L^{-1} led to a reduction in CO_2 emission (20.04 and 12.94 mg 24 h^{-1} g^{-1}, respectively) (Fig. 5d). At 1 g L^{-1}, only ZAE significantly increased SBR compared to the other concentrations (26.4 mg 24 h^{-1} g^{-1}), whereas the other ZnO NPs showed a decreasing trend (Fig. 5d). Regarding concentration, 0.5 g L^{-1} showed the highest level of microbial activity, and the effects of ZnO NPs on microbial activity were ranked as follows: ZNB > ZSB > chemically synthesized ZnO NPs > ZAE > ZNE > ZAB > ZSE.

The effect of ZnO NPs on the carbon activity of soil microbiota was assessed in calcareous soils to determine its overall effects on microbial activity. Overall, the alteration in soil microbial respiration in soils treated with ZnO NPs

was significant (Fig. 5d). Soil respiration potential decreased at a ZnO NPs loading rate of 0.5 g L^{-1} and at 1 g L^{-1} of ZnO NPs, although it remained significantly different from the control (Fig. 5d). Research conducted by Ge et al. (2012) indicated that low levels of ZnO NPs have a modest effect on enhancing the basal respiration rates of soil microorganisms. We hypothesized that zinc directly contributes to the enhancement of SBR by stimulating microbial respiration, as Zn is a vital element for all organisms. CO_2 levels observed in treatments with 150 and 300 mg kg^{-1} of ZnO NPs were greater than those recorded for 1 and 10 mg kg^{-1} in soil. The elevated levels of nano-ZnO NPs create stress among microorganisms, resulting in an increase in CO_2. Consequently, we determined that a suitable dose of nano-ZnO has the potential to enhance SBR.

Zhou et al. (2020) reported an increase in the abundance of *Gemmatimonas* with increasing zinc concentrations. Changes in *Gemmatimonas* abundance suggest that ZnO NPs increases environmental stress on soil microorganisms and causes changes in the abundance of metal-oxidizing bacteria. On the other hand, the CO_2 emission rate was inhibited only by a high dose of ZnO NPs (500 mg kg^{-1}) (García-Gómez et al., 2018), which is consistent with our findings. At a treatment level of 1000 mg kg^{-1} ZnO NPs, the respiration rate in calcareous soil was significantly reduced (García-Gómez et al., 2018). Huang et al. (2022) showed that the response of soil microbial communities to the application of ZnO NPs is highly diverse and depends on the characteristics of the system and the form of Zn applied.

Moreover, zinc solubility is inversely related to the pH and clay content in calcareous soil, which facilitates greater retention of Zn within the soil matrix. This situation reduces the availability of Zn to microorganisms. Clays have the capacity to adsorb Zn^{2+} through ion exchange and specific adsorption (Jiang et al., 2021). The presence of Zn is also related to soil organic matter (SOM). The effect of SOM content on Zn availability to microorganisms should be considered small, as the amounts present in the soil are very low (< 2%) (Ge et al., 2012). The investigation of nanotoxicity in soil presents significant challenges and complexities due to the numerous interactions between NPs and their surrounding environment, as well as the relationships between NPs and microorganisms.

Table 2. Growth pattern of plant growth-promoting rhizobacteria (PGPR) exposed to different concentrations of ZnO NPs.

ZnO NPs Type	ZnO NPs conc. (mg ml^{-1})	PGPR			
		Micrococcus yunnanensis	***Pseudomonas fluorescens***	***Azospirillum***	***Bacillus subtilis***
ZNE	10	MIC	(-)MBC	(-)MBC	(-)MBC
	5	+	MIC	MIC	(-)MBC
	2.5	+	+	+	(-)MBC
	1.25	+	+	+	MIC
	0.625	+	+	+	+
ZSE	10	MIC	MIC	+	(-)MBC
	5	MIC	MIC	+	MIC
	2.5	+	MIC	+	MIC
	1.25	+	MIC	+	MIC
	0.625	+	+	+	+
ZAE	10	+	MIC	(-)MBC	(-)MBC
	5	+	MIC	MIC	(-)MBC
	2.5	+	+	+	MIC
	1.25	+	+	+	MIC
	0.625	+	+	+	+
ZNB	10	+	MIC	(-)MBC	(-)MBC
	5	+	+	MIC	(-)MBC
	2.5	+	+	MIC	MIC
	1.25	+	+	+	+
	0.625	+	+	+	+
ZSB	10	MIC	MIC	MIC	MIC
	5	MIC	MIC	MIC	MIC
	2.5	+	MIC	+	+
	1.25	+	+	+	+
	0.625	+	+	+	+
ZAB	10	+	MIC	(-)MBC	(-)MBC
	5	+	MIC	MIC	MIC
	2.5	+	MIC	+	+
	1.25	+	MIC	+	+
	0.625	+	+	+	+
ZO	10	+	MIC	MIC	(-)MBC
	5	+	MIC	MIC	MIC
	2.5	+	MIC	MIC	MIC
	1.25	+	+	MIC	+
	0.625	+	+	MIC	+

Positive (+): indicating growth and negative (-): indicating absence of growth; MIC: minimum inhibitory concentration, MBC: minimum bactericidal concentration, PGPR: plant growth-promoting rhizobacteria, ZnO NPs: zinc oxide nanoparticles, ZNE:

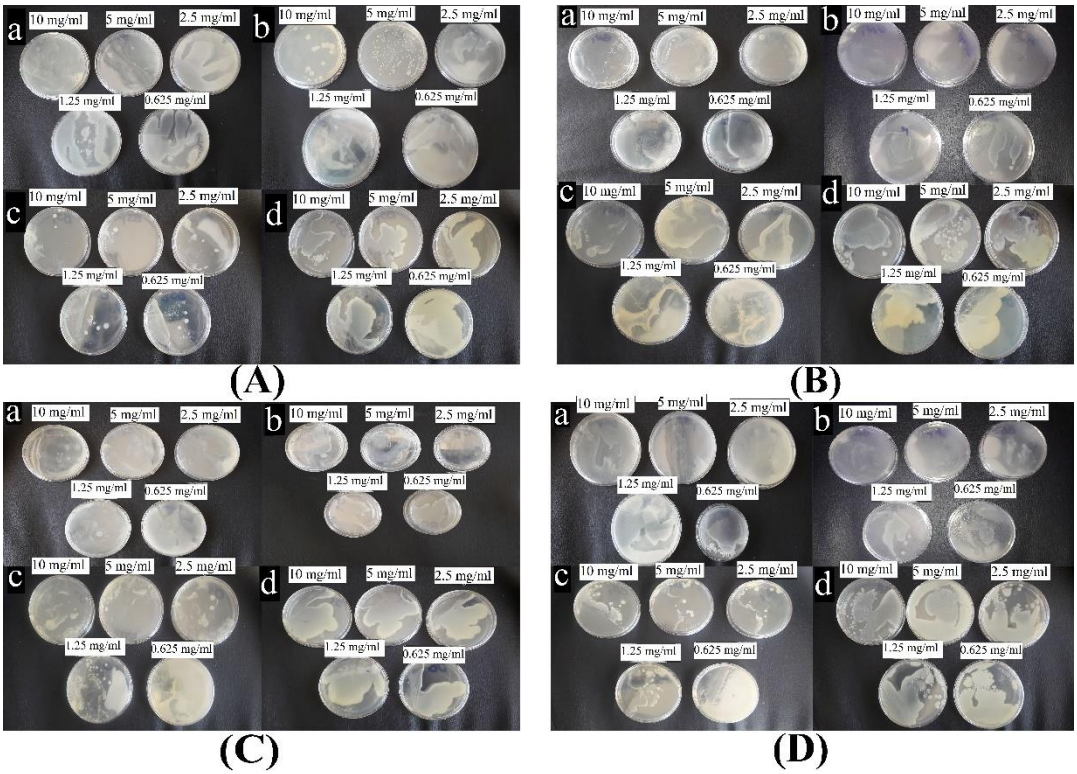

Escherichia coli-Zn$(NO_3)_2$, ZSE: *Escherichia coli*-$ZnSO_4$, ZAE: *Escherichia coli*-Zn$(CH_3COO)_2$, ZNB: *Bacillus subtilis*-Zn (NO3)2, ZSB: *Bacillus subtilis*-$ZnSO_4$, ZAB: *Bacillus subtilis*-Zn $(CH3COO)_2$, and ZO: chemically synthesized ZnO.

Fig. 7. Growth pattern of (a) *Bacillus subtilis*, (b) *Azospirillum*, (c) *Pseudomonas fluorescens*, and (d) *Micrococcus yunnanensis* at several doses of ZnO NPs (A*: Bacillus subtilis*-Zn $(NO_3)_2$, B: *Bacillus subtilis*-$ZnSO_4$, C: *Bacillus subtilis*-Zn $(CH_3COO)_2$, and D: chemically synthesized ZnO) onto nutrient agar plates, 24 h post incubation at 37 °C.

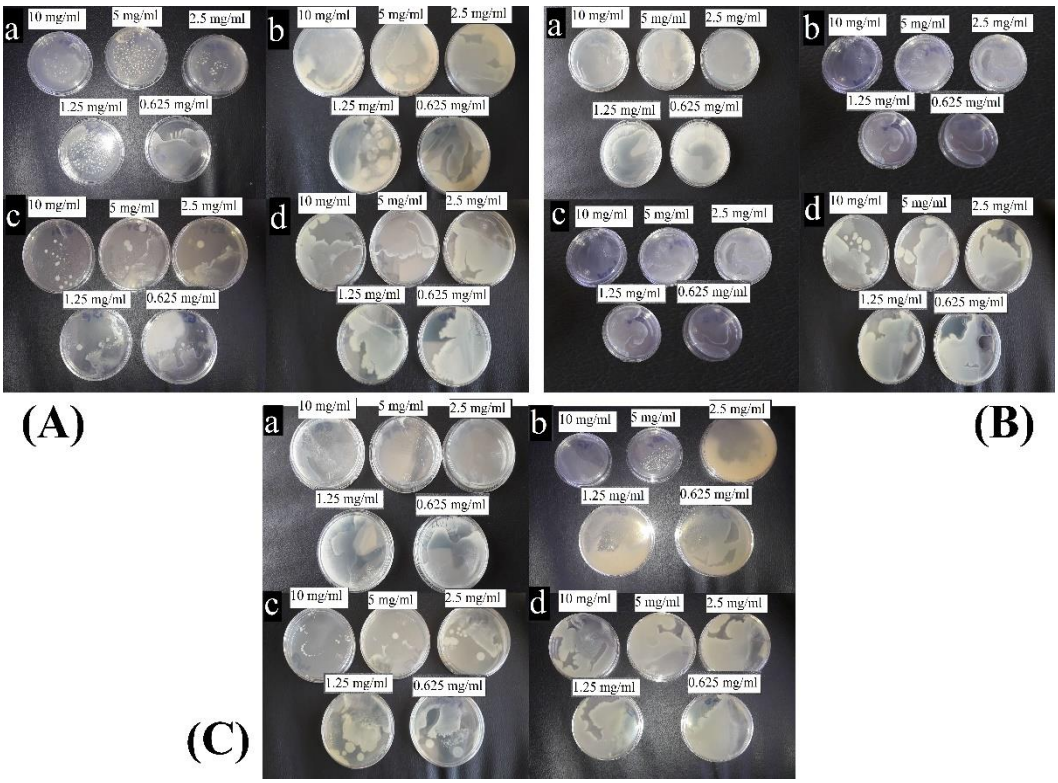

Fig. 8. Growth pattern of (a) *Bacillus subtilis*, (b) *Azospirillum*, (c) *Pseudomonas fluorescens*, and (d) *Micrococcus yunnanensis* at different doses of ZnO NPs (A: *Escherichia coli*-Zn $(NO_3)_2$, B: *Escherichia coli*-$ZnSO_4$, and C: *Escherichia coli*-Zn $(CH_3COO)_2$) onto nutrient agar plates 24 h post incubation at 37 °C.

Nonetheless, chemically synthesized NPs have certain limitations, including the generation of toxic by-products that can be harmful to the environment. Furthermore, these reactions generally require significant energy input and frequently incur substantial costs associated with the acquisition of chemicals (Sarkhosh et al., 2022). Consequently, it is essential to develop methods for synthesizing NPs that are cost-effective, environmentally-friendly, and biocompatible. Biosynthesis has emerged as a viable alternative and a solution to the difficulties posed by chemical processes (Singh et al., 2023). The application of bio-extracts reduces environmental impacts while also enabling different compounds to form a coating on the surface of the generated NPs, which subsequently improves their properties and performance (Sánchez-Pérez et al., 2023). Therefore, NPs generated through green synthesis are more desirable than those synthesized chemically.

CONCLUSION

In the present study, we reported that the precursor salt and bacterial strain are two of the most important factors that directly affect NP biosynthesis. The production of ZnO NPs with different sizes and properties was a result of these two variables. ZnO NPs were observed to have spherical shapes and sizes ranging from 28 to 600 nm based on TEM micrographs and DLS, while the stabilization of ZnO NPs by coating proteins in the bacterial supernatant was confirmed by FTIR spectra. The present findings suggest that ZnO NPs may improve seed vigor, germination, and maize seedling growth when 0.1 g L^{-1} ZnO NPs was biosynthesized via *B. subtilis* and *E. coli* using $ZnSO_4$ through seed priming in water. The application of ZnO NPs synthesized by *B. subtilis* and *E. coli* increased maize shoot and root dry weight, regardless of the Zn source. The optimal response of ZnO NPs in relation to soil basal respiration was observed at 0.5 g L^{-1}. Also, ZnO NPs biosynthesized by *B. subtilis* using $ZnSO_4$ and $Zn(NO_3)_2$ promoted beneficial effects compared to the control and chemically synthesized ZnO NPs. The 0.625 mg mL^{-1} dose of ZnO NPs showed lower bactericidal activity against PGPR. Chemically synthesized ZnO NPs were most capable of inhibiting PGPR growth, whereas ZnO NPs that were made using *B. subtilis* and $Zn(NO_3)_2$ showed lower efficiency in inhibiting PGPR growth at 1.25 mg mL^{-1}. Particle size and characteristics play important roles. Thus, the reactivity of NPs requires careful consideration when determining the appropriate concentration for application, as high doses may reduce seed growth and PGPR activity. In addition, the negative effects of biologically synthesized ZnO NPs were less than those of chemically synthesized ZnO NPs. In contrast to chemical or physical methods, the biosynthesis of ZnO NPs is widely known as being more environmentally-friendly.

FUNDING

This research was funded by Shiraz University, grant number 3GCB1M154659.

CRediT AUTHORSHIP CONTRIBUTION STATEMENT

Conceptualization: Mehdi Zarei and Amir Ghafar Shahriari; Methodology: Narges Abdar; Software: Narges Abdar; Validation: Mehdi Zarei and Amir Ghafar Shahriari; Formal analysis: Narges Abdar; Investigation: Mehdi Zarei and Narges Abdar; Resources: Narges Abdar; Data curation: Narges Abdar; Writing—original draft preparation: Narges Abdar; Writing—review and editing: Mehdi Zarei, Reza Ghasemi, Alireza Afsharifar, Amir Ghafar Shahriari, and Narges Abdar; Visualization: Mehdi Zarei, Amir Ghafar Shahriari, and Narges Abdar; Supervision: Mehdi Zarei; Project administration: Mehdi Zarei; Funding acquisition: Mehdi Zarei, Amir Ghafar Shahriari, and Narges Abdar. All authors have read and agreed to the published version of the manuscript.

DECLARATION OF COMPETING INTEREST

The authors declare no conflicts of interest.

ETHICAL STATEMENT

Not applicable

DATA AVAILABILITY

The data provided are uploaded as a supplementary file and are made freely available upon request by readers.

ACKNOWLEDGMENTS

Shiraz University (Shiraz, Iran) provided funding for this study.

REFERENCES

Ahmad, A., Ullah, S., Syed, F., Tahir, K., Khan, A. U., & Yuan, Q. (2020). Biogenic metal nanoparticles as a potential class of antileishmanial agents: Mechanisms and molecular targets. *Nanomedi*, *15*, 809-828. https://doi.org/10.2217/nnm-2019-0413

Ahmadian, E., Eftekhari, A., Kavetskyy, T., Khosroushahi, A. Y., Turksoy, V. A., & Khalilov, R. (2020). Effects of quercetin loaded nanostructured lipid carriers on the paraquat-induced toxicity in human lymphocytes. *Pesticide Biochemistry and Physiology*, *167*, 104586. https://doi.org/10.1016/j.pestbp.2020.104586

Akintelu, S. A., & Folorunso, A. S. (2020). A review on green synthesis of zinc oxide nanoparticles using plant extracts and its biomedical applications. *BioNanoScience*, *10*, 848-863. https://doi.org/10.1007/s12668-020-00774-6

Ali, J., Irshad, R., Li, B., Tahir, K., Ahmad, A., Shakeel, M., & Khan, Z. U. H. (2018). Synthesis and characterization of phytochemical fabricated zinc oxide nanoparticles with enhanced antibacterial and catalytic applications. *Journal of Photochemistry and Photobiology*, *183*, 349-356. https://doi.org/10.1016/j.jphotobiol.2018.05.006

Al-Kordy, H. M., Sabry, S. A., & Mabrouk, M. E. (2021). Statistical optimization of experimental parameters for extracellular synthesis of zinc oxide nanoparticles by a

novel haloalaliphilic Alkalibacillus sp. W7. *Scientific Reports*, *11*, 10924. https://doi.org/10.1038/s41598-021-90408-y

Almoneef, M. M., Awad, M. A., Aldosari, H. H., Hendi, A. A., Aldehish, H. A., Merghani, N. M., & Alshammari, S. G. (2024). Exploring the multi-faceted potential: Synthesized ZnO nanostructure–Characterization, photocatalysis, and crucial biomedical applications. *Heliyon*, *10*, 1-15. https://doi.org/10.1016/j.heliyon.2024.e32714

Ameen, F., Alsamhary. K., Alabdullatif, J. A., & ALNadhari, S. (2021). A review on metal-based nanoparticles and their toxicity to beneficial soil bacteria and fungi. *Ecotoxicology and Environmental Safety*, *213*, 112027. https://doi.org/10.1016/j.ecoenv.2021.112027

Aslam, A. A., Aslam, M. S., & Aslam, A. A. (2022). An overview on green synthesis of nanoparticles and their advanced applications in sustainable agriculture. *International Journal of Biology and Chemistry*, *3*(2), 70-99. https://doi.org/10.20944/preprints202202.0315.v1

Chikezie, I. O. (2017). Determination of minimum inhibitory concentration (MIC) and minimum bactericidal concentration (MBC) using a novel dilution tube method. *African Journal of Microbiology Research*, *11*, 977-980. https://doi.org/10.5897/AJMR2017.8545

Duhan, J. S., Kumar, R., Kumar, N., Kaur, P., Nehra, K., & Duhan, S. (2017). Nanotechnology: The new perspective in precision agriculture. *Biotechnology reports*, *15*, 11-23. https://doi.org/10.1016/j.btre.2017.03.002

El-ghwas, D. E. (2022). Characterization and biological synthesis of zinc oxide nanoparticles by new strain of Bacillus *Biodiversitas Journal of Biological Diversity*, *23*(1), 1-6. https://doi.org/10.13057/biodiv/d230159

El-Nour, A., Amira, T., Abou-Dobara, M. I., El-Sayed, A. K., & El-Zahed, M. M. (2023). Extracellular biosynthesis and antimicrobial activity of *Bacillus subtilis* ATCC 6633 zinc oxide nanoparticles. *Scientific Journal for Damietta Faculty of Science*, *13*(2), 39-47. https://doi.org/10.21608/SJDFS.2023.173178.1064

Esper Neto, M., Britt, D. W., Lara, L. M., Cartwright, A., dos Santos, R. F., Inoue, T. T., & Batista, M. A. (2020). Initial development of corn seedlings after seed priming with nanoscale synthetic zinc oxide. *Agron*, *10*, 307. https://doi.org/10.3390/agronomy10020307

Fakhari, S., Jamzad, M., & Kabiri Fard, H. (2019). Green synthesis of zinc oxide nanoparticles: A comparison. *Green Chemistry Letters and Reviews*, *12*, 19-24. https://doi.org/10.1080/17518253.2018.1547925

Fakhri, N., Salehnia, F., Mohammad Beigi, S., Aghabalazadeh, S., Hosseini, M., Ganjali, M. R. (2019). Enhanced peroxidase-like activity of platinum nanoparticles decorated on nickel-and nitrogen-doped graphene nanotubes: colorimetric detection of glucose. *Microchimica Acta*, *186*, 1-9. https://doi.org/10.1007/s00604-019-3489-3

García-Gómez, C., Fernández, M. D., García, S., Obrador, A. F., Letón, M., & Babín, M. (2018). Soil pH effects on the toxicity of zinc oxide nanoparticles to soil microbial community. *Environmental Science and Pollution Research*, *25*, 28140-28152. https://doi.org/10.1007/s11356-018-2833-1

Ge, Y., Schimel, J. P., & Holden, P. A. (2012). Identification of soil bacteria susceptible to TiO_2 and ZnO nanoparticles. *Applied and Environmental Microbiology*, *78*, 6749-6758. https://doi.org/10.1128/AEM.00941-12

Hamk, M., Akçay, F. A., & Avcı, A. (2023). Green synthesis of zinc oxide nanoparticles using *Bacillus subtilis* ZBP4 and their antibacterial potential against foodborne pathogens. *Preparative Biochemistry and Biotechnology*, *53*, 255-264. https://doi.org/10.1080/10826068.2022.2076243

Huang, H., Chen, J., Liu, S., & Pu, S. (2022). Impact of ZnO nanoparticles on soil lead bioavailability and microbial properties. *Science of the Total Environment*, *80*, 150-299. https://doi.org/10.1016/j.scitotenv.2021.150299

Hudlikar, M., Joglekar, S., Dhaygude, M., & Kodam, K. (2012). Latex-mediated synthesis of ZnS nanoparticles: Green synthesis approach. *Journal of Nanoparticle Research*, *14*, 1-6. https://doi.org/10.1007/s11051-012-0865-x

Jiang, H., Yang, B., Wang, H., Chen, Q., Cao, X., Gao, Y., & Yin, K. (2021). Insights on the effects of ZnO nanoparticle exposure on soil heterotrophic respiration as revealed by soil microbial communities and activities. *Journal of Soils and Sediments*, *21*, 2315-2326. https://doi.org/10.1007/s11368-021-02947-6

Khajeh, M., & Golzary, A. R. (2014). Synthesis of zinc oxide nanoparticles–chitosan for extraction of methyl orange from water samples: Cuckoo optimization algorithm–artificial neural network. *Spectrochimica Acta Part A: Molecular and Biomolecular Spectroscopy*, *131*, 189-194. https://doi.org/10.1016/j.saa.2014.04.084

Khana I., Saeed K., Khanc I. (2019). Nanoparticles: Properties, applications and toxicities. *Arabian Journal of Chemistry*, *12*, 908 -931. https://doi.org/10.1016/j.arabjc.2017.05.011

Kwak, J. I., Yoon, S. J., & An, Y. J. (2017). Long-term effects of ZnO nanoparticles on exoenzyme activities in planted soils. *Environmental Engineering Research*, *22*, 224-229. https://doi.org/10.4491/eer.2016.103

Liu, X., Wang, F., Shi, Z., Tong, R., & Shi, X. (2015). Bioavailability of Zn in ZnO nanoparticle-spiked soil and the implications to maize plants. *Journal of Nano Research*, *17*, 1-11. https://doi.org/10.1007/s11051-015-2989-2

Mohmed, A. A., Fouda, A., Abdel-Rahman, M. A., El-Din Hassan, S., El-Gamal, M. S., Salem, S. S., & Shaheen, T. I. (2019). Fungal strain impacts the shape, bioactivity and multifunctional properties of green synthesized zinc oxide nanoparticle, *Biocatalysis and Agricultural Biotechnolog*, *19*, 101103. https://doi.org/10.1016/j.bcab.2019.101103

Mohd Yusof, H., Mohamad, R., Zaidan, U. H., & Abdul Rahman, N. A. (2019). Microbial synthesis of zinc oxide nanoparticles and their potential application as an antimicrobial agent and a feed supplement in animal industry: A review. *Journal of Animal Science and Biotechnology*, *10*, 1-22. https://doi.org/10.1186/s40104-019-0368-z

Munir, T., Rizwan, M., Kashif, M., Shahzad, A., Ali, S., Amin, N., Zahid, R., Alam, M. F. E., & Imran, M. (2018). Effect of zinc oxide nanoparticles on the growth and Zn uptake in wheat (*Triticum aestivum* L.) by seed priming method. *Digest Journal of Nanomaterials and Biostructures*, *13*, 315-323.

Nasrollahzadeh, M., Sajjadi, M., Sajadi, S. M., & Issaabadi, Z. (2019). Green nanotechnology. *Interface Science and Technology*, *28*, 145-198. https://doi.org/10.1016/B978-0-12-813586-0.00005-5

Nkabinde, S. S., Mathebula, X., Tetana, Z., & Moloto, N. (2018). The role of zinc metal salts on size, morphology and photocatalytic activity of ZnO. *MRS Advances*, *3*, 2653-2665. https://doi.org/10.1557/adv.2018.209

Omar, A. A., Heikal, Y. M., Zayed, E. M., Shamseldin, S. A., Salama, Y. E., Amer, K. E., & Mohamed, A. H. (2023). Conferring of drought and heat stress tolerance in wheat (*Triticum aestivum* L.) genotypes and their response to selenium nanoparticles application. *Nanomaterials*, *13*(6), 998. https://doi.org/10.3390/nano13060998

Pourrahimi, A. M., Liu, D., Pallon, L. K., Andersson, R. L., Abad, A. M., Lagarón, J. M., & Olsson, R. T. (2014). Water-based synthesis and cleaning methods for high purity ZnO nanoparticles–comparing acetate, chloride, sulphate and nitrate zinc salt precursors. *RSC Advances*, *4*, 35568-35577. https://doi.org/10,1039/C4RA06651K

Priester, J. H., Ge, Y., Mielke, R. E., Horst, A. M., Moritz, S. C., Espinosa, K., & Holden, P. A. (2012). Soybean susceptibility to manufactured nanomaterials with evidence for food quality and soil fertility interruption. *Proceedings of the National Academy of Sciences*, *109*, E2451-E2456. https://doi.org/10.10773/pnas.1205431109

Raj, A., & Lawerence, R. (2018). Green synthesis and charcterization of zno nanoparticles from leafs extracts of rosa indica and its antibacterial activity. *Nutriation*, *11*, 1339-1348. http://dx.doi.org/10.31788/RJC.2018.1132009

Ranum, P., Peña-Rosas, J. P., & Garcia-Casal, M. N. (2014). Global maize production, utilization, and consumption. *Annals of the New York Academy of Sciences*, *1312*, 105-112. https://doi.org/10.1111/nyas.12396.

Rehman, S., Jermy, B. R., Akhtar, S., Borgio, J. F., Abdul Azeez, S., Ravinayagam, V., & Gani, A. (2019). Isolation and characterization of a novel thermophile; Bacillus haynesii, applied for the green synthesis of ZnO nanoparticles. *Artificial Cells, Nanomedicine, and Biotechnology*, *47*, 2072-2082. https://doi.org/10.1080/21691401.2019.1620254

Rizvi, A., & Khan, M. S. (2018). Heavy metal induced oxidative damage and root morphology alterations of maize (*Zea mays* L.) plants and stress mitigation by metal tolerant nitrogen fixing *Azotobacter chroococcum*. *Ecotoxicology and Environmental Safety*, *157*, 9-20. https://doi.org/10.1016/j.ecoenv.2018.03.063

Sabir, S., Zahoor, M. A., Waseem, M., Siddique, M. H., Shafique, M., Imran, M., & Muzammil, S. (2020). Biosynthesis of ZnO nanoparticles using Bacillus subtilis: characterization and nutritive significance for promoting plant growth in *Zea mays* L. *Dose-Response*, *18*, 1559325820958911. https://doi.org/10.1177/1559325820958911

Salman, J. A. S., Kadhim, A. A., & Haider, A. J. (2018). Biosynthesis, characterization and antibacterial effect of ZnO nanoparticles synthesized by *Lactobacillus* Spp. *Journal of Global Pharma Technology*, *10*, 348-355.

Sánchez-Pérez, D. M., Márquez-Guerrero, S. Y., Ramírez-Moreno, A., Rodríguez-Sifuentes, L., Galindo-Guzmán, M., Flores-Loyola, E., & Marszalek, J. E. (2023). Impact of biologically and chemically synthesized zinc oxide nanoparticles on seed germination and seedlings' growth. *Horticul*, *9*, 1201. https://doi.org/10.3390/horticulturae9111201

Sarkhosh, S., Kahrizi, D., Darvishi, E., Tourang, M., Haghighi-Mood, S., Vahedi, P., & Ercisli, S. (2022). Effect of zinc oxide nanoparticles (ZnO-NPs) on seed germination characteristics in two brassicaceae family species: *Camelina sativa* and *Brassica napus* L. *Journal of Nanomaterials*, *2022*(1), 1892759. https://doi.org/10.1155/2022/1892759

Siddhardha Busi, S. B., Jobina Rajkumari, J. R., Subhaswaraj Pattnaik, S. P., Paramanandham Parasuraman, P. P., & Sairengpuii Hnamte, S. H. (2016). Extracellular synthesis of zinc oxide nanoparticles using *Acinetobacter schindleri* SIZ7 and its antimicrobial property against foodborne pathogens. *Journal of microbiology, biotechnology and food sciences*, *5*(5), 407-411. https://doi.org/10.15414/jmbfs.2016.5.5.407-411

Simonin, M., & Richaume, A. (2015). Impact of engineered nanoparticles on the activity, abundance, and diversity of soil microbial communities: A review. *Environmental Science and Pollution Research*, *22*, 13710-13723. https://doi.org/10.1007/s11356-015-4171-x

Singh, D. K., Pandey, D. K., Yadav, R. R., & Singh, D. (2012). A study of nanosized zinc oxide and its nanofluid. *Pramana*, *78*, 759-766. https://doi.org/10.1007/s12043-012-0275-8

Singh, J., Kumar, S., Alok, A., Upadhyay, S. K., Rawat, M., Tsang, D. C., & Kim, K. H. (2019). The potential of green synthesized zinc oxide nanoparticles as nutrient source for plant growth. *Journal of Cleaner Production*, *214*, 1061-1070. https://doi.org/10.1016/j.jclepro.2019.01.018

Singh, N. A., Narang, J., Garg, D., Jain, V., Payasi, D., Suleman, S., & Swami, R. K. (2023). Nanoparticles synthesis via microorganisms and their prospective applications in agriculture. *Plant Nano Biology*, *5*, 100047. https://doi.org/10.1007/s12043-012-0275-8

Solís-Sandí, I., Cordero-Fuentes, S., Pereira-Reyes, R., Vega-Baudrit, J. R., Batista-Menezes, D., de Oca-& Vásquez, G. M. (2023). Optimization of the biosynthesis of silver nanoparticles using bacterial extracts and their antimicrobial potential. *Biotechnology Reports*, *40*, e00816. https://doi.org/10.1016/j.btre.2023.e00816

Srivastav, A., Ganjewala, D., Singhal, R. K., Rajput, V. D., Minkina, T., Voloshina, M., & Shrivastava, M. (2021). Effect of ZnO nanoparticles on growth and biochemical responses of wheat and maize. *Plants*, *10*, 2556. https://doi.org/10.3390/plants10122556

Suganya, A., Saravanan, A., & Manivannan, N. (2020). Role of zinc nutrition for increasing zinc availability, uptake, yield, and quality of maize (*Zea mays* L.) grains:

An overview. *Communications in Soil Science and Plant Analysi*, *51*, 2001-2021. https://doi.org/10.1080/00103624.2020.1820030

Suhad, H., Neihaya, H. Z., & Raghad, A. L. (2021). Evaluating the biological activities of biosynthesized ZnO nanoparticles using *Escherichia coli*. *Caspian Journal of Environmental Sciences*, *19*, 809-815. https://doi.org/10.22124/CJES.2021.5221

Thakur, S., Neogi, S., & Ray, A. K. (2021). Morphology-controlled synthesis of ZnO nanostructures for caffeine degradation and *Escherichia coli* inactivation in water. *Catalysts*, *11*, 63. https://doi.org/10.3390/catal11010063

Tripathi, D. K., Singh, S., Singh, S., Mishra, S., Chauhan, D. K., & Dubey, N. K. (2015). Micronutrients and their diverse role in agricultural crops: Advances and future prospective. *Acta Physiologiae Plantarum*, *37*, 1-14. https://doi.org/10.1007/s11738-015-1870-3

Umar, W., Hameed, M. K., Aziz, T., Maqsood, M. A., Bilal, H. M., & Rasheed, N. (2021). Synthesis, characterization and application of ZnO nanoparticles for improved growth and Zn biofortification in maize. *Archives of Agronomy and Soil Science*, *67*, 1164-1176. https://doi.org/10.1080/03650340.2020.1782893

Wagner, G., Korenkov, V., Judy, J. D., & Bertsch, P. M. (2016). Nanoparticles composed of Zn and ZnO inhibit Peronospora tabacina spore germination in vitro and P. tabacina infectivity on tobacco leaves. *Nanomaterials*, *6*, 50. https://doi.org/10.3390/nano6030050.

Wilpiszeski, R. L., Aufrecht, J. A., Retterer, S. T., Sullivan, M. B., Graham, D. E., Pierce, E. M., & Elias, D. A. (2019). Soil aggregate microbial communities: Towards understanding microbiome interactions at biologically relevant scales. *Applied and Environmental Microbiology*, *85*, 19-24. https://doi.org/10.1128/AEM.00324-19

Yadav, R., Kumar, M., Tomar, R. S. (2023). Revisiting the microbial biosynthesis of metal nanoparticles and their applications. *Journal of Applied Pharmaceutical Science*, *13*, 013-031. https://doi.org/10.7324/JAPS.2023.89282

Zhang, L., Wu, L., Si, Y., & Shu, K. (2018). Size-dependent cytotoxicity of silver nanoparticles to Azotobacter vinelandii: Growth inhibition, cell injury, oxidative stress and internalization. *PloS one*, *13*(12), e0209020. https://doi.org/10.1371/journal.pone.0209020

Zhao, L., Hernandez-Viezcas, J. A., Peralta-Videa, J. R., Bandyopadhyay, S., Peng, B., Munoz, B., & Gardea-Torresdey, J. L. (2013). ZnO nanoparticle fate in soil and zinc bioaccumulation in corn plants (*Zea mays*) influenced by alginate. *Environmental Science: Processes and Impacts*, *15*, 260-266. https://doi.org/10.1039/C2EM30610G

Zhou, Q., Zhang, X., Wu, Z. (2020). Impact of TiO_2 and ZnO nanoparticles on soil bacteria and the enantioselective transformation of racemic-metalaxyl in agricultural soil with Lolium perenne: A wild greenhouse cultivation. *Journal of Agricultural and Food Chemistry*, *68*, 11242-11252. https://doi.org/10.1021/acs.jafc.0c03959